

Mucin Granule Intraluminal Organization in Living Mucous/Goblet Cells

ROLES OF PROTEIN POST-TRANSLATIONAL MODIFICATIONS AND SECRETION^{*[5]}

Received for publication, September 26, 2005, and in revised form, December 22, 2005 Published, JBC Papers in Press, December 23, 2005, DOI 10.1074/jbc.M510520200

Juan Perez-Vilar^{‡1}, Raean Mabolo[‡], Cheryl T. McVaugh[§], Carolyn R. Bertozzi^{§¶||**}, and Richard C. Boucher[‡]

From the [‡]Cystic Fibrosis/Pulmonary Research and Treatment Center, University of North Carolina, Chapel Hill, North Carolina 27599-7248, the Departments of [§]Chemistry and [¶]Molecular and Cell Biology, University of California, Berkeley, California 94720, and the ^{||}Howard Hughes Medical Institute and the ^{**}Material Sciences Division, Lawrence Berkeley National Laboratory, Berkeley, California 94720-1460

Recent studies suggest that the mucin granule lumen consists of a matrix meshwork embedded in a fluid phase. Secretory products can both diffuse, although very slowly, through the meshwork pores and interact noncovalently with the matrix. Using a green fluorescent protein-mucin fusion protein (SHGFP-MUC5AC/CK) as a FRAP (fluorescence recovery after photobleaching) probe, we have assessed in living mucous cells the relative importance of different protein post-translational modifications on the intragranular organization. Long term inhibition of mucin-type *O*-glycosylation, sialylation, or sulfation altered SHGFP-MUC5AC/CK characteristic diffusion time ($t_{1/2}$), whereas all but sulfation diminished its mobile fraction. Reduction of protein disulfide bonds with tris(hydroxypropyl)phosphine resulted in virtually complete immobilization of the SHGFP-MUC5AC/CK intragranular pool. However, when activity of the vacuolar H⁺-ATPase was also inhibited, disulfide reduction decreased SHGFP-MUC5AC/CK $t_{1/2}$ while diminishing its intraluminal concentration. Similar FRAP profiles were observed in granules that remained in the cells after the addition of a mucin secretagogue. Taken together these results suggest that: (a) the relative content of *O*-glycans and intragranular anionic groups is crucial for protein diffusion through the intragranular meshwork; (b) protein-protein, rather than carbohydrate-mediated, interactions are responsible for binding of SHGFP-MUC5AC/CK to the immobile fraction, although the degree of matrix *O*-glycosylation and sialylation affects such interactions; (c) intragranular organization does not depend on covalent multimerization of mucins or the presence of native disulfide bonds in the intragranular mucin/proteins, but rather on specific protein-mediated interactions that are important during the early stages of mucin matrix condensation; (d) alterations of the intragranular matrix precede granule discharge, which can be partial and, accordingly, does not necessarily involve the disappearance of the granule.

In response to specific signals, regulated secretion permits the controlled transport of membrane and secretory products (1, 2). This pathway is supported by an efficient mechanism for importing/packing proteins into secretory granules. Indeed, the biogenesis of regulated secretory granules is initiated when secretory proteins aggregate in the *trans*-Golgi compartments (3). Nevertheless, our understanding of intragranular protein condensation and its regulation still is fragmented and incomplete, especially in exocrine cells.

Mucous/goblet cells are specialized in the synthesis and (constitutive/regulated) secretion of a family of glycoproteins known as secreted gel-forming mucins (4–7). Mucins are characterized by their large size, high degree of mucin-type *O*-glycosylation, and the formation of disulfide-linked oligomers/multimers. Together with water and salts, mucins largely determine the viscoelastic and adhesive properties of the mucus secretions that cover the tracheobronchial, gastrointestinal, urogenital, auditory, and conjunctival epithelia. Although the mucus layer lubricates and protects epithelial cells against pathogenic and noxious agents (8, 9), overproduction of mucus can be detrimental to health, as is evident in lung diseases characterized by a mucus hypersecretory phenotype such as cystic fibrosis (10).

The biosynthesis of mucins comprises *N*- and *O*-glycosylation, likely *C*-mannosylation, sulfation, interchain disulfide bond formation, and proteolysis (6, 11–13). Processed mucin oligomers/multimers are stored inside mucin granules, where they likely form a highly condensed polyanionic matrix (14–17). Consistent with this notion, intestinal mucous cells with the characteristic mucin granules are not present in mice lacking expression of *mMuc2*, the gene encoding the major intestinal gel-forming mucin (18). Polyanionic matrices and high intraluminal concentrations of Ca²⁺ and H⁺ appear to be common features of regulated secretory granules irrespective of species and the cell type (e.g. 1, 19–21). Ca²⁺ and H⁺ likely shield the negative charges in mucin *O*-linked oligosaccharide chains, facilitating the emergence of physical interactions among intragranular matrix mucins. It has been proposed that at some point during granule biogenesis, and following the same physical laws that govern phase transitions of synthetic polymers (22), polyanionic intragranular proteins in general, and mucin oligomers/multimers in particular, undergo a highly cooperative (likely Ca²⁺/H⁺-driven) phase transition (condensation) process, which results in the formation of osmotically inert, condensed aggregates (16, 17, 23). Moreover, an ion exchange (Ca²⁺/K⁺)-triggered phase transition of the matrix is thought to occur prior to and/or during granule exocytosis, resulting in matrix decondensation and hydration and discharge of entrapped secretory proteins (24, 25).

Recent studies in live mucous/goblet cells have revealed novel aspects on mucous/goblet cells and their granules (26, 27). Thus, fluorescence

* This work was supported by Cystic Fibrosis Foundation Grants PEREZ310 and PEREZV04G0 (to J. P.-V.), National Institutes of Health Grants DK63030 (to J. P.-V.) and GM66047 (to C. R. B.), and the Prostate Cancer Development Research Program Prostate SPOR Award P50 CA89520 (to C. R. B.). Parts of this work were presented at the 2004 and 2005 Meetings of the Biophysical Society in Baltimore, Maryland, and Long Beach, California, respectively. The costs of publication of this article were defrayed in part by the payment of page charges. This article must therefore be hereby marked "advertisement" in accordance with 18 U.S.C. Section 1734 solely to indicate this fact. This manuscript is dedicated to the memory of Dr. A. Paradiso, University of North Carolina at Chapel Hill.

[5] The online version of this article (available at <http://www.jbc.org>) contains supplemental Figs. s1–s3.

¹ To whom correspondence should be addressed: Cystic Fibrosis/Pulmonary Research and Treatment Center, CB7248, University of North Carolina at Chapel Hill, Chapel Hill, NC 27599-7248. Tel.: 919-843-5142; Fax: 919-966-7524; E-mail: juan_vilar@med.unc.edu.

recovery after photobleaching (FRAP)² analyses with a mucin-GFP fusion protein suggested that the mucin granule lumen is compartmentalized into a mobile or fluid phase, in which secretory products diffused very slowly, and an immobile, pH-dependent phase (*i.e.* a “matrix”) to which secretory products were noncovalently bound via pH-dependent interactions (26). A two-phase, intraluminal organization was proposed independently on the basis of studies on the Ca²⁺/K⁺ intragranular ion exchange mechanism of exocytosis (28, 29). The facts that the same protein probe diffused ~100-fold faster in the endoplasmic reticulum lumen than within the mucin granule, whereas its diffusion seemed even faster once it reached the extracellular mucus³ (26), supports the notion that the intragranular mucin matrix is in a condensed state. However, the FRAP profiles obtained argued against the existence of an inaccessible, dehydrated condensed mucin matrix surrounded by a dense fluid phase (26). Instead, the mucin meshwork is likely embedded in a fluid phase so that proteins diffuse through its pores and have access to, and interact with, the matrix components. Although these studies are not necessarily in conflict with a phase transition-driven mechanism of matrix condensation, they raise the possibility that specific protein-protein interactions have critical roles at some point during the formation of the matrix meshwork.

Using time-lapse and semiquantitative FRAP analysis in live mucous cells, we report here studies aimed at identifying the relative roles in mucin granule organization of mucin post-translational modifications, including O-glycosylation, sulfation, sialylation, and protein disulfide bonding. The intraluminal environment of granules remaining after the addition of mucin secretagogue was also investigated. The results suggest that the intragranular environment can be independently regulated by different factors.

EXPERIMENTAL PROCEDURES

Maintenance of HT29-SHGFP-MUC5AC/CK Cells and Experimental Treatments—The generation, characterization, and maintenance of HT29-SHGFP-MUC5AC/CK cells were described earlier (26). Compound 2-68A (100 μg/ml; Ref. 31), sodium chlorate (10 mg/ml; Ref. 32), 4-methylumbelliferyl-β-D-xylopyranoside (10 mM; Ref. 33), the peptides NH₂-GNWVWW and NH₂-WRGGSG (100 μM; Ref. 34), denoted herein as P6SIAL and P6CON, respectively, tris(hydroxypropyl)phosphine (THP, 5 mM, Calbiochem; Ref. 35), bafilomycin A₁ (0.1 μg/ml; Ref. 36) or dithiothreitol (DTT, 5 mM; Ref. 37) were freshly prepared in culture medium, with solubilization in dimethyl sulfoxide when required, and given to the cells for 48 h, in the case of compound 2-68A and sodium chlorate or 72 h in the case of 4-methylumbelliferyl-β-D-xylopyranoside, P6SIAL or P6CON. To induce mucin granule secretion, cells were incubated for at least 30 min in the presence of 3 mM ATP prior to FRAP or biochemical analysis. In all cases, vehicle-incubated control cells were analyzed in parallel under the same conditions. Unless otherwise indicated, all of the reagents and peptides mentioned in this work were obtained from Sigma.

Generation of NIH-3T3-SHGFP-MUC5AC/CK Cells—NIH-3T3 cells, obtained from ATCC and maintained as directed by the provider, were transduced with a retroviral vector encoding SHGFP-MUC5AC/CK essentially as described earlier for HT29-18N2 cells (26). After selection in puromycin-containing culture medium, the cells were maintained for at least 20 passages prior to use for these studies. At

that point, this cell line did not differ from the parental cell line regarding morphologic features and growth rate.

Confocal Microscopy and FRAP Analysis—Cells in confocal medium (Hanks' balanced solution salt plus 1% (v/v) fetal bovine serum, 5 mM L-glutamine, essential and nonessential amino acids, and 20 mM HEPES, pH 7.8) were observed with a Zeiss LSM 510 (University of North Carolina Michael Hooker Microscopy Facility) at 37 °C on the microscope stage, using 488 nm laser excitation for GFP. FRAP analysis of intragranular SHGFP-MUC5AC/CK in live mucous/goblet cells was carried out using a ×63 (NA 1.4) oil immersion objective as described before (26). Briefly, a spot the size of the laser beam diameter was irreversibly bleached and the fluorescence intensity in the bleached area monitored over time. From these raw data, the mobile fraction (*M_f*), *i.e.* the percent of intragranular SHGFP-MUC5AC/CK that diffuses, and the characteristic diffusion time (*t_{1/2}*), *i.e.* the time required to reach 50% of the plateau fluorescence in the bleached area, were derived using standard procedures (26, 38). In each case, vehicle- and compound-treated cells were analyzed in parallel. At least three different culture dishes from three independent experiments were processed. The statistical significance of differences between the means of specific parameters in specific pairs of vehicle- and compound-treated cells was assessed by student *t* tests.

Caspase 3/7 Assays—To assess the cellular levels of caspases 3 and 7, cells grown in 4-well slides (Cultek, Inc.) were put on ice for 5 min, washed twice with cold Ca²⁺/Mg²⁺-free PBS, and lysed for 15 min at room temperature in 300 μl of 0.5% (v/v) Triton X-100 in PBS/well. The lysates were cleared by centrifugation at 16,000 × *g* for 1 min and then diluted 1:100 with sterile water. 1–10 μl of the latter solution was mixed with an equal volume of freshly made caspase 3/7-Glo reagent (Promega, Inc.). The mixture was incubated at room temperature for up to 1 h and light emission measured with a Turner Biosystem 20/20 luminometer.

Analysis of Glycoproteins Metabolically Labeled with N-Acetyl-³H]Glucosamine or ³⁵SO₄Na₂—Mucous cells grown in 35-mm culture dishes were metabolically labeled at 37 °C with 25 μCi/ml N-acetyl-³H]glucosamine (³H]GlcNAc, Amersham Biosciences; 35 Bq/mmol) or 50 μCi/ml ³⁵SO₄Na₂ (MPB; 74 MBq) in PFHM-II culture medium (39) for 24 h in the absence (control sample) or presence of the indicated compounds. At the end of the labeling, the cells were put on ice for 5 min and the culture medium collected and cleared from cell debris by centrifugation. The cell layer was rinsed with cold PBS and then extracted at 4 °C with 4 M guanidine HCl, 0.1 M sodium acetate, 4% (w/v) CHAPS, 100 μM phenylmethylsulfonyl fluoride, pH 5.8 (extraction buffer; 3 ml/dish), for 30 min with agitation. The lysates were cleared by centrifugation and the supernatant diluted with extraction buffer to a concentration of 0.5–0.7 mg of protein/ml. Radioactive proteins were separated from unincorporated radioactive probe by passing 500 μl of cell lysate through a 5-ml Sephadex G-50 (fine) column equilibrated in 6 M urea, 0.1 M Tris-HCl, 5 mM EDTA, 0.5% CHAPS (w/v), 100 μM phenylmethylsulfonyl fluoride, pH 8.0 (elution buffer). The proteins were eluted with elution buffer and 0.5-ml fractions collected. The radioactivity in each fraction was measured by scintillation counting.

To determine the incorporation of the radioactive label into high molecular weight glycoproteins/mucins, cell lysates were dialyzed against 6 M urea, 0.1 M Tris-HCl, 5 mM EDTA, pH 8.0, for 18 h at 4 °C, then reduced with 20 mM DTT for 18 h at room temperature and carbonylmethylated with freshly prepared 20 mM iodoacetamide for 30 min at 25 °C in the dark (40). Proteins (30 μg/well) were separated and visualized by standard gradient (4–20%) SDS-PAGE and fluorography. Alternatively, proteins were separated in 1% SDS-agarose gels as described previously (40), and equal square pieces (~0.5 × 0.5 cm²)

² The abbreviations used are: FRAP, fluorescence recovery after photobleaching; CHAPS, 3-[(3-cholamidopropyl)dimethylammonio]-1-propanesulfonic acid; DTT, dithiothreitol; GFP, green fluorescent protein; *M_f*, mobile fraction; PBS, phosphate-buffered saline; SiaNAc, sialic acid; *t_{1/2}*, half-recovery time or characteristic diffusion time; THP, tris(hydroxypropyl)phosphine.

³ J. Perez-Vilar, unpublished observations.

Mucin Granule Intraluminal Organization

were cut from the top to the bottom of the agarose gels. The gel pieces were melted with guanidine thiocyanate, pH 8, at 65 °C for 10 min and mixed with 2.5 ml of Safety Solve prior to counting the total radioactivity in a scintillation counter.

Protein Blotting of Endogenous MUC5AC Separated in Agarose Gels—Total cellular proteins were extracted, separated by SDS-agarose gel electrophoresis, transferred to nitrocellulose membranes, and MUC5AC detected with specific antibodies following published procedures (40). A mouse anti-human MUC5AC monoclonal antibody (2Q445; U. S. Biologicals) recognizing the unglycosylated tandem repeat region of MUC5AC (41), and a specific rabbit antiserum, named MUC5AC-062, obtained against a peptide (TWTTWFDVDFPS) of the MUC5AC Cys-5 subdomain, respectively, were employed in these studies. As judged by protein blotting, this antiserum specifically detects the same molecular species of MUC5AC recognized by another well characterized rabbit anti-MUC5AC (41), including cystine-reduced, unglycosylated, and *O*-glycosylated monomers, but not unreduced species of this mucin (not shown).

Other Methods—Cellular DNA was purified from cell extracts using the DNeasy Tissue kit from Qiagen and its concentration estimated by absorbance at 260 nm. Protein concentration was determined by the bicinchoninic acid assay using reagents from Pierce. The sialic acid content in cultures of HT29-SHGFP-MUC5AC/CK cells was assessed by microscopy using SNA-biotin (Vector Laboratories) as the specific label. Thus, cells were fixed with methanol at -20 °C, nonspecific binding sites blocked with 10% (w/v) bovine serum albumin in PBS, and sialic acid residues located with SNA-biotin (0.05 μg/ml in PBS) and streptavidin-rhodamine. XY serial images of the cultures were obtained via confocal microscopy.

RESULTS

Inhibition of Mucin-type *O*-Glycosylation Alters SHGFP-MUC5AC/CK Intragranular Mobile Fraction and Mobility—Mucin-type *O*-glycosylation is the major post-translational modification of gel-forming mucins, and it can represent up to 90% of their molecular weights (4). To assess the relative importance of this modification in intragranular organization, *O*-glycosylation was inhibited in HT29-SHGFP-MUC5AC/CK mucous intestinal adenocarcinoma cells (26). These cells stably express SHGFP-MUC5AC/CK, a fusion protein consisting of a secreted form of GFP and the CK domain of MUC5AC, one of the five human gel-forming mucins known. SHGFP-MUC5AC/CK does not covalently bind to endogenous MUC5AC, but it is stored inside the mucin granules (26). To inhibit *O*-glycosylation, cells were grown in the presence of compound 2-68A. This uridine derivative is a specific competitive inhibitor of the UDP-GalNAc:polypeptide α -GalNAc-transferase family of glycosyltransferases that initiate mucin-type *O*-glycosylation (31). Cultures incubated with vehicle (dimethyl sulfoxide) (Fig. 1A, *a* and *b*) or compound 2-68A (*c* and *d*) appeared to have comparable number of mucous cells with numerous mucin granules each (Fig. 1B), suggesting that compound 2-68A was not toxic under these conditions.

Because it has been reported that inhibition of *O*-glycosylation by uridine derivatives triggers cellular apoptosis in different cell types (31, 42), it was important to assess whether the degree of cellular apoptosis differed between control and 2-68A-incubated cultures. Thus, the activities of caspases 3 and 7, two well characterized apoptosis markers (43), were determined in cell lysates of mucous cells incubated for 48 h in the presence of vehicle or compound 2-68A. As shown in Fig. 1C, the respective cellular levels of caspase 3/7 were very similar, suggesting that under these experimental conditions, compound 2-68A did not induce

apoptosis. To validate these results, we generated NIH-3T3 cells stably expressing SHGFP-MUC5AC/CK, the same protein expressed by the mucous cell line. NIH-3T3 is a cell line known to undergo apoptosis upon inhibition of *O*-glycosylation with uridine derivatives (42). Consistent with these reports, the addition of compound 2-68A to NIH-3T3-SHGFP-MUC5AC/CK fibroblasts resulted in increased caspase 3/7 activities within an hour (Fig. 1D) and widespread and extensive cellular apoptosis 24 h later (Fig. 1E).

The effectiveness of compound 2-68A as an *O*-glycosylation inhibitor in mucous cells was assessed by determining the incorporation of a radioactive monosaccharide into cellular glycoproteins. In these studies, cells preincubated for 24 h with vehicle (dimethyl sulfoxide) or compound 2-68A were metabolically labeled with [³H]GlcNAc for another 24 h in the presence of dimethyl sulfoxide or compound 2-68A. ³H-Labeled proteins from cell lysates were separated from unincorporated radioactive monosaccharide by gel filtration and the radioactivity in each fraction quantified. Compared with control cells, cells incubated with compound 2-68A had a much smaller signal in the excluded volume fractions (Fig. 1F), which contain proteins eluted from the column. Similarly, compound 2-68A inhibited incorporation of [³H]GlcNAc into high molecular weight glycoproteins/mucins fractionated by SDS-agarose gel electrophoresis (see supplemental Fig. s1). Consistent with these results, the cellular binding of SNA, a lectin specific for sialic acid residues, was reduced in compound 2-68A-treated cells (see supplemental Fig. s2). These results are consistent with substantial inhibition of mucin type *O*-glycosylation by compound 2-68A in cultured mucous cells, as has been reported in other cell types treated with uridine derivatives *in vitro* and *in vivo* (31, 42).

Having provided experimental evidence that mucin-type *O*-glycosylation was inhibited efficiently, whereas the mucous cells were not apoptotic, we analyzed the intragranular FRAP parameters in granules from vehicle- or compound 2-68A-incubated living mucous cells processed in parallel. Because the inhibitor was added to cultures in which *in vitro* mucous cell differentiation was already in progress (26, 39), we expected that after 2 days with the inhibitor, a significant fraction of underglycosylated mucins and other glycoproteins would be present within the granules. A spot of ~0.26-μm radius in mucin granules with diameters equal to or larger than 1.1 μm was photobleached, and the recovery of the fluorescence within the bleach spot followed over time (26). Similar to control granules (26), in the presence of compound 2-68A intraluminal SHGFP-MUC5AC/CK was fractionated between a mobile and an immobile phase (Fig. 2A). However, as judged from the normalized raw FRAP curves, 2-68A-incubated granules had a lower asymptotic recovery value than control granules, suggesting a smaller SHGFP-MUC5AC/CK M_f . Indeed, the differences between their respective mean M_f values were statistically significant ($p < 0.01$; Fig. 2B).

SHGFP-MUC5AC/CK intragranular characteristic diffusion times or half-recovery times ($t_{1/2}$) were determined after photobleaching from the respective normalized, corrected fluorescence recovery curves fitted to a one-phase exponential equation (26, 38). In both cases, a wide range of $t_{1/2}$ values were obtained (Fig. 2C), consistent with previous studies (26), although the differences in their respective mean $t_{1/2}$ values indicated that compound 2-68A significantly ($p < 0.01$) increased SHGFP-MUC5AC/CK mobility. Altogether these results suggest that mucin-type *O*-glycosylation influences both binding of SHGFP-MUC5AC/CK to the intragranular matrix and its mobility through the granule fluid phase.

Inhibition of Protein Sulfation Increases SHGFP-MUC5AC/CK Intragranular Mobility—Intragranular polyanionic matrix proteins appear to be a critical feature for packing and unpacking of secretory products

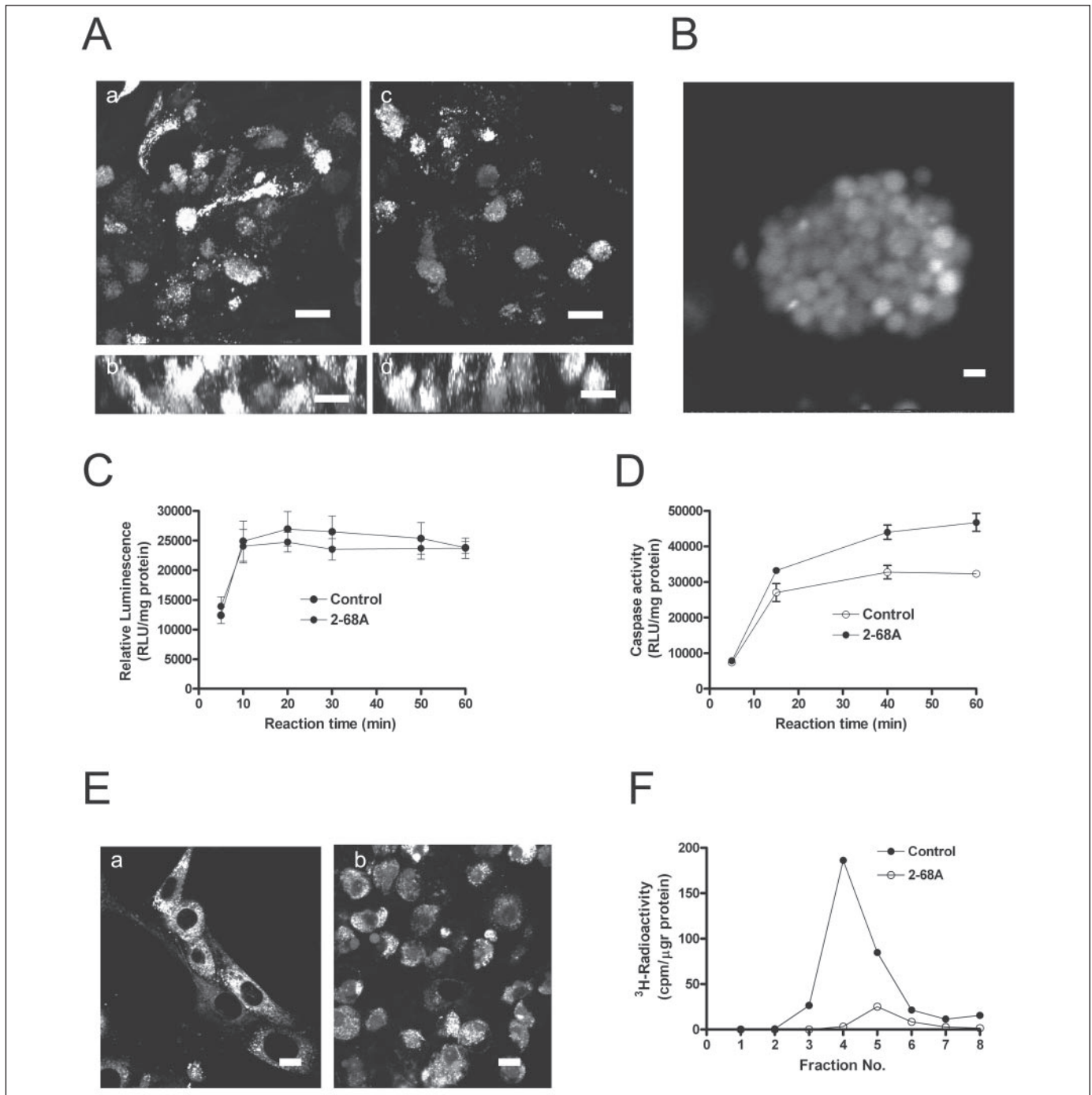


FIGURE 1. Degree of apoptosis and [³H]GlcNAc protein incorporation in cells incubated with compound 2-68A. *A*, representative *xy* (*a* and *c*) or *xz* (*b* and *d*) confocal images of live HT29-SHGFP-MUC5AC/CK cells incubated for 48 h in vehicle (*a* and *b*) or compound 2-68A (*c* and *d*). Scale bar = 10 μm. *B*, representative mucous/goblet cell from a cell culture incubated in the presence of compound 2-68A. Scale bar = 2 μm. *C*, activity levels of caspases 3/7 per μg of total protein in cell lysates of HT29-SHGFP-MUC5AC/CK cells, previously incubated for 48 h with vehicle (*Control*) or compound 2-68A. The graph shows the mean (± S.E.) values obtained with three independent cultures as a function of the reaction time. Error bars indicate S.E. *D*, specific activity levels of caspases 3/7 in NIH-3T3 cell lysates obtained as in *C* except that cells were incubated with vehicle (*Control*) or compound 2-68A for 4 h. Error bars indicate S.E. *E*, representative *xy* confocal images of live NIH-3T3 cells incubated for 24 h in vehicle (*a*) or compound 2-68A (*b*). Notice that in the presence of 2-68A, the cells lost their characteristic fibroblast morphology, becoming smaller and with widespread membrane blebbing and cell fragmentation/vesiculation. Scale bar = 5 μm. *F*, representative result of studies assessing the incorporation of [³H]GlcNAc into cellular glycoproteins of HT29-SHGFP-MUC5AC/CK cells incubated with vehicle or compound 2-68A. Cell extracts were fractionated in a Sephadex G-50 column, the radioactivity (cpm) in each fraction determined, and the results divided by the total protein in the respective cell extracts.

(17–20). Considering the effects of compound 2-68A and that sulfation and sialylation of *O*-glycans endow mucins with their characteristic anionic nature (4), we wanted to assess the relative importance of these two modifications for intraluminal organization in mucin granules. Here we describe experiments aimed at inhibiting protein sulfation,

whereas studies on the inhibition of sialylation are described in the next subsection.

To reduce intragranular sulfation, we incubated mucous cells for 48 h in the presence of sodium chlorate, a well established inhibitor of the biosynthesis of 3'-phosphoadenosine 5'-phosphosulfate, the universal sulfate

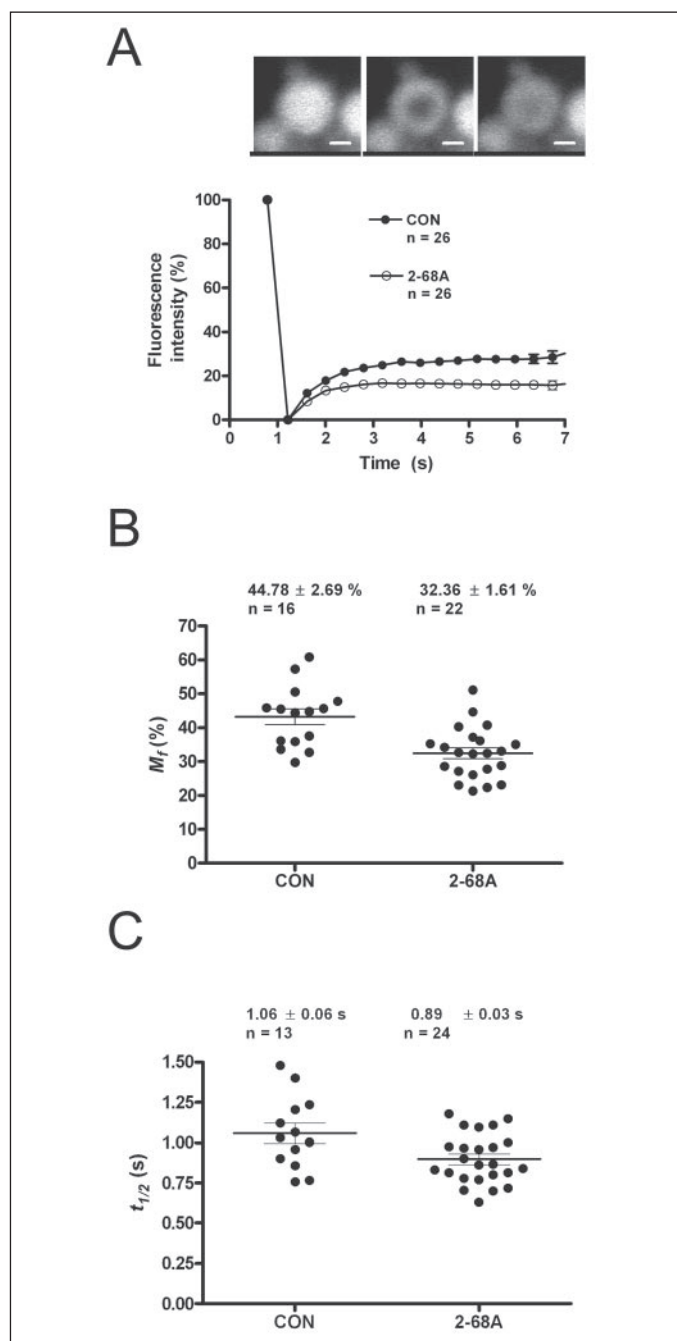


FIGURE 2. Mobile fraction and mobility of intragranular SHGFP-MUC5AC/CK in live mucous cells incubated with compound 2-68A. *A*, averaged (mean ± S.E.) normalized FRAP bleaching/recovery curves for 26 granules each of vehicle- (CON) and compound 2-68A-incubated cells, respectively. Error bars indicate S.E. A representative mucin granule in a 2-68A-incubated live goblet cell, showing pre- (left), immediately post- (center), and 7 s postbleaching (right) confocal images is shown at the top of the plot. Scale bar = 0.5 μ m. *B*, scatter plot of SHGFP-MUC5AC/CK intragranular M_f in control (CON) and 2-68A-treated live mucous/goblet cells. The respective M_f mean values (±S.E.) are shown. *C*, scatter plot of SHGFP-MUC5AC/CK intragranular $t_{1/2}$ in control and 2-68A-incubated live mucous/goblet cells. The respective $t_{1/2}$ mean values (±S.E.) are shown.

donor (32). In the presence of chlorate, the percent of mucous cells and the number of granules/cell were similar to control cells (Fig. 3A). These results are consistent with previous studies, suggesting that inhibition of mucin sulfation with sodium chlorate does not affect the rate and amount of mucin secretion (32). FRAP curves showed that in chlorate-treated granules, SHGFP-MUC5AC/CK was fractionated between a mobile and an immobile phase, similar to granules in control cells (Fig. 3B). Although the

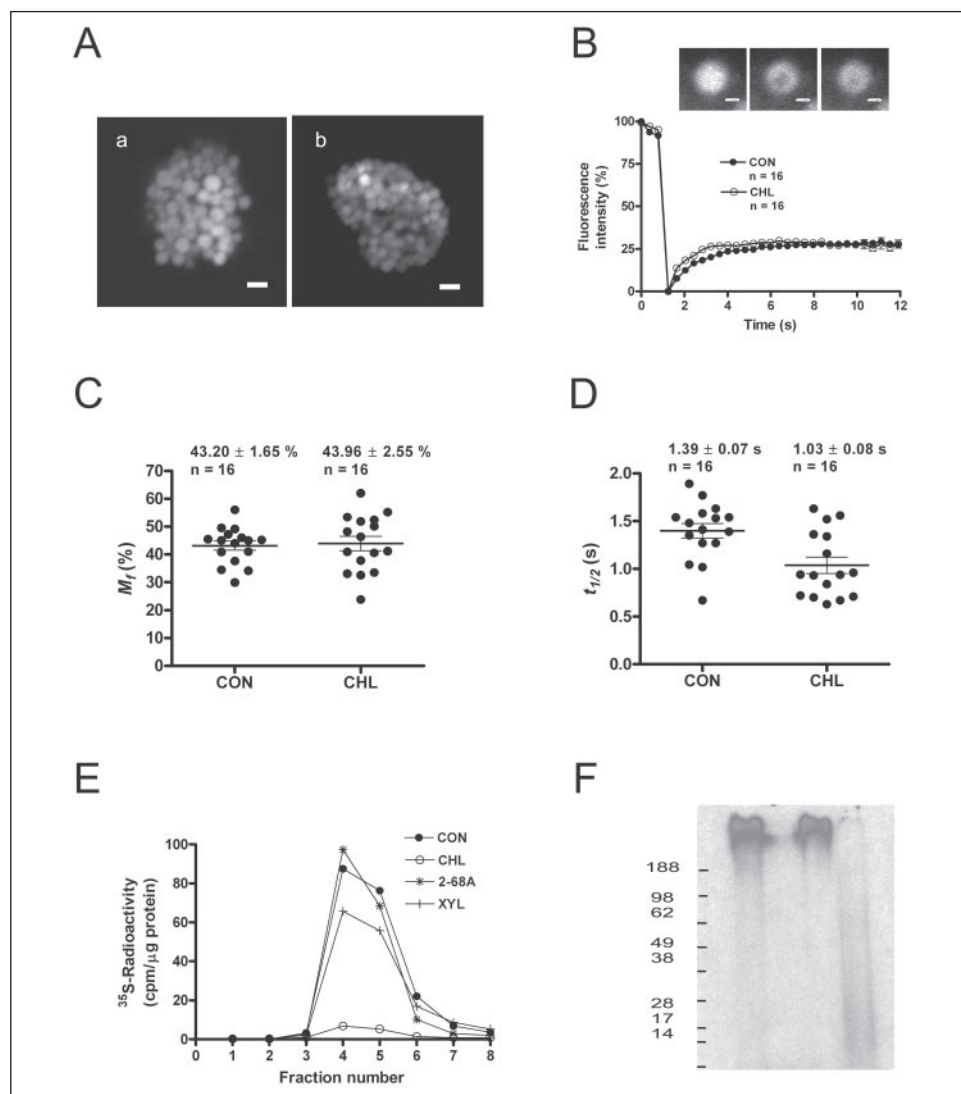
recovery plateau was reached earlier in chlorate-treated than in untreated granules, they both shared the same asymptotic value. Consistent with these observations, the difference between their respective mean M_f values was not statistically significant ($p = 0.551$; Fig. 3C). Conversely, the difference between their mean $t_{1/2}$ values was statistically significant ($p < 0.005$; Fig. 3D). These results indicated that SHGFP-MUC5AC/CK intragranular mobility was inversely related to the intragranular content of sulfate groups.

To assess the relative contribution of mucin-type O-glycans and xylose-containing glycosaminoglycan chains to the cellular synthesis of $^{35}\text{SO}_4$ -labeled proteins, mucous cells were incubated with compound 2-68A or 4-methylumbelliferyl- β -D-xylopyranoside to inhibit mucin-type O-glycosylation or glycosaminoglycan biosynthesis (33), respectively. After 24 h, the culture medium was replaced with fresh medium containing the respective compound and, in addition, $^{35}\text{SO}_4\text{Na}_2$, and the cells incubated for another 24 h. ^{35}S -Labeled proteins were extracted from cell lysates and separated from unincorporated $^{35}\text{SO}_4\text{Na}_2$ by gel filtration. Although the radioactivity in the excluded fraction of protein extracts from chlorate- and xyloside-incubated cells dropped to ~92% and ~23% ($n = 3$) of the value of control extracts, respectively, the corresponding values from cells incubated with compound 2-68A only diminished ~8% (Fig. 3E).

Separation of DTT-reduced samples in 4–20% gradient SDS-polyacrylamide gels (Fig. 3F) corroborated these results and also suggested that high molecular weight sulfated proteoglycans were the major cellular sulfated glycoproteins. Thus, $^{35}\text{SO}_4$ incorporation was (a) largely confined to proteins that penetrated the stacking but not the resolving gel (lane 1); (b) inhibited by chlorate (lane 2) and xyloside (lane 4); and (c) only very slightly decreased by compound 2-68A (lane 3). In the presence of xyloside (lane 4), a diffuse smear of ^{35}S -labeled material appeared throughout the bottom half of the gels. This smear likely resulted from xyloside-primed sulfated glycosaminoglycan chains synthesized in the cells (33) that were coeluted from the gel filtration columns with the ^{35}S -labeled proteins. Immunoblotting with anti-MUC5AC 062 antiserum showed that MUC5AC penetrated the top of these gels (data not shown). These results showed that sulfation in HT29-SHGFP-MUC5AC/CK cells was effectively arrested by sodium chlorate and suggested that their high molecular weight glycoproteins/mucins were poorly sulfated, consistent with studies indicating that colon cancer mucins are undersulfated (44). Hence the changes in SHGFP-MUC5AC/CK mobility in the presence of sodium chlorate were likely caused by diminished sulfation of high molecular weight, xylose-containing intragranular proteoglycans. Purification of SHGFP-MUC5AC/CK by metal affinity chromatography from $^{35}\text{SO}_4$ -labeled protein extracts suggested that the single N-glycan oligosaccharide chain in the fusion protein (26) was not sulfated (data not shown).

Inhibition of Sialyltransferases Reduces the Intragranular Mobility and Mobile Fraction of SHGFP-MUC5AC/CK—To alter protein sialylation, mucous cells were incubated in medium containing the hexapeptide GDW WWW (P6SIAL). This peptide, which is an *in vitro* competitive inhibitor of all sialyltransferases involved in the biosynthesis of N- and O-linked oligosaccharides (34), has been shown earlier to be an effective inhibitor of protein sialylation when added to cultured mammalian cells (34). To test whether P6SIAL was also an effective inhibitor in HT29-SHGFP-MUC5AC/CK mucous cells, we prepared chemically fixed cells and used confocal microscopy to assess the binding of the sialic acid-specific lectin SNA. Control cells processed in parallel were incubated with the hexapeptide WRGGSG (P6CON), which does not inhibit sialyltransferases (34). As shown in Fig. 4A, lectin binding in control cells (a) clearly

FIGURE 3. Mobile fraction and mobility of intragranular SHGFP-MUC5AC/CK in live mucous cells incubated with sodium chlorate. *A*, *xy* confocal images of a representative control (*a*) and a sodium chlorate-treated (*b*) live mucous/goblet cell, respectively. Scale bars = 1 μm . *B*, averaged (mean \pm S.E.) normalized FRAP bleaching/recovery curves for 16 granules each of control (CON) and sodium chlorate (CHL)-treated cells. Error bars indicate S.E. A representative mucin granule in a 2-68A-treated live goblet cell, showing pre- (*left*), immediately post- (*center*), and 10 s postbleaching (*right*) confocal images is shown at the top of the plot. Scale bar = 0.5 μm . *C*, scatter plot of SHGFP-MUC5AC/CK intragranular M_f in control and sodium chlorate-treated live mucous/goblet cells. The respective M_f mean values (\pm S.E.) are shown. *D*, scatter plot of SHGFP-MUC5AC/CK intragranular $t_{1/2}$ in control and sodium chlorate-treated live mucous/goblet cells. The respective $t_{1/2}$ mean values are shown. *E*, representative result of studies assessing the degree of incorporation of ^{35}S into cellular proteins of HT29-SHGFP-MUC5AC/CK cells incubated with control, sodium chlorate, compound 2-68A, or xyloside (XYL). Cell extracts were fractionated in a Sephadex G-50 column, the radioactivity (cpm) in each fraction determined, and the results divided by the total protein in the respective extracts. *F*, ^{35}S -labeled cellular proteins of mucous cells previously incubated with vehicle (*lanes 1 and 2*), sodium chlorate (*lane 2*), compound 2-68A (*lane 3*), or xyloside (*lane 4*) were separated in 4–20% gradient SDS-polyacrylamide gels after reduction of disulfide bonds with DTT. Protein bands were detected by fluorography. *MWM*, molecular mass markers, which are given in kDa; *SG*, stacking gel; *RG*, resolving gel.



decreased in P6SIAL-treated cells (*b*), with a reduction of $\sim 35\%$ in the mean intensity/pixel. These results showed that P6SIAL was an effective protein sialylation inhibitor in mucous cells.

The percent of mucous cells and the number of granules/cell appeared the same as in control cells (Fig. 4*B*). Moreover, diminished sialylation did not prevent intragranular fractionation of SHGFP-MUC5AC/CK between a mobile and an immobile phase, similar to granules in control cells, as judged by FRAP (data not shown). However, the intragranular mean M_f value of SHGFP-MUC5AC/CK was smaller ($p < 0.005$) in the presence of P6SIAL than with P6CON in the culture medium (Fig. 4*C*), suggesting that reduction of sialic residues increased the binding of SHGFP-MUC5AC/CK to the mucin matrix. In addition, P6SIAL increased ($p < 0.004$) the fusion protein $t_{1/2}$ mean value over control cells (Fig. 4*D*), which indicates that its intragranular mobility decreased when sialyltransferases were inhibited.

Reduction of Disulfide Bonds Alters the Intraluminal Organization of Mucin Granules—The FRAP analyses of mucin granules in live mucous cells are consistent with a three-dimensional meshwork-like organization of the intraluminal immobile fraction/matrix (26). This kind of organization might involve, in addition to electrostatic links between sialylated/sulfated *O*-glycans in mucins and multivalent cations (16, 17), specific protein-protein interactions between mucin oligomers. In this

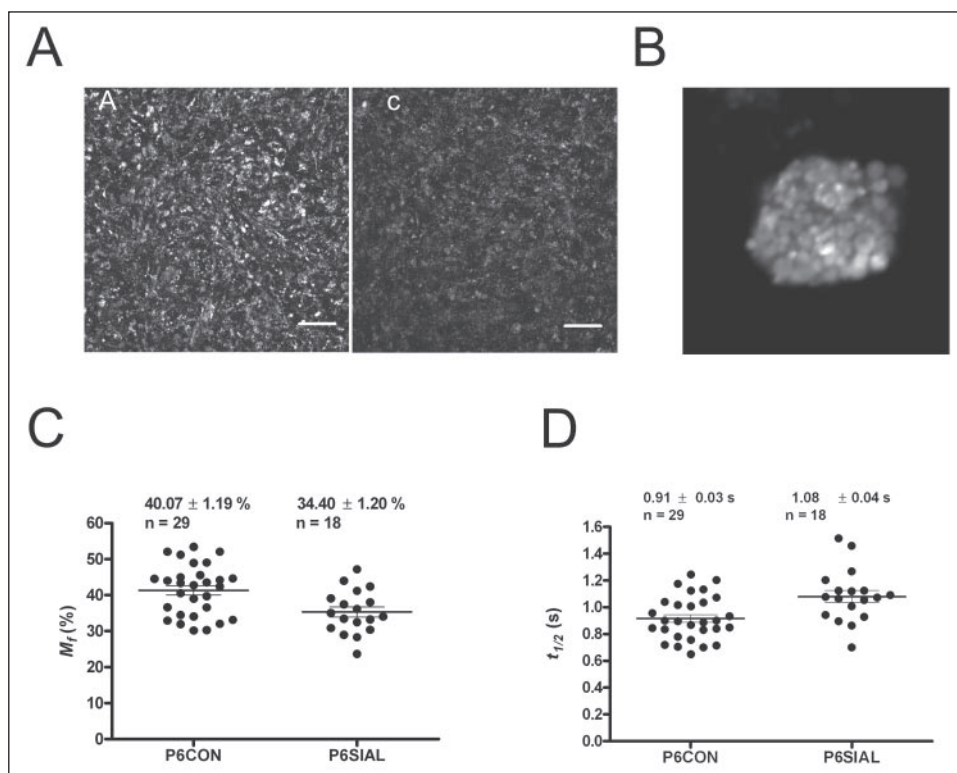
respect, formation of intra- and interchain disulfide bonds are critical steps during the folding and multimeric assembly of gel-forming mucins (6) and would be expected to influence noncovalent homo- and heterotypic interactions.

To assess the importance of intragranular protein disulfide bonds in mucin granule organization, we incubated mucous cells with THP, a cell-permeable, disulfide reducing agent effective at acidic pH (35). Preliminary studies showed that THP was well tolerated by HT29 mucous cells at concentrations of up to 5 mM when added to regular culture medium for 5 h or less. Higher concentrations or longer incubation periods resulted in cell detachment.

The efficiency of THP was evaluated by analyzing the oxidation status of intragranular MUC5AC, the major gel-forming mucin synthesized and secreted by HT29 cells (45). Cellular proteins were extracted under nonreducing conditions from control or THP-incubated cells and reacted with iodoacetamide to prevent oxidation of cysteine residues (40). Another protein sample from control extracts was reduced with DTT and reacted with iodoacetamide. Proteins were separated in SDS-agarose gels, transferred to nitrocellulose membranes, and detected by Western blotting with antiserum MUC5AC-062. This antiserum recognizes native MUC5AC in which disulfide bonds are reduced, similar to a well characterized

Mucin Granule Intraluminal Organization

FIGURE 4. Mobile fraction and mobility of intragranular SHGFP-MUC5AC/CK in live mucous cells incubated with P6SIAL. *A*, three-dimensional projection of 12 xy confocal images comprising the entire cellular layer of HT29-SHGFP-MUC5AC/CK cells incubated for 48 h in the presence of P6CON (*a*) or P6SIAL (*b*). The cells were fixed with methanol and stained with SNA-biotin/streptavidin-rhodamine. Scale bar = 20 μ m. *B*, xy confocal image of a representative living mucous/goblet cell incubated for 48 h in the presence of P6SIAL. Scale bar = 3 μ m. *C*, scatter plot of SHGFP-MUC5AC/CK intragranular M_f in mucous cells incubated for 72 h with a control peptide (P6CON) or P6SIAL. The respective mean values (\pm S.E.) are shown. Error bars indicate S.E. *D*, scatter plot of SHGFP-MUC5AC/CK intragranular $t_{1/2}$ in control (P6CON) and P6SIAL-treated live mucous/goblet cells. Error bars indicate S.E. The respective $t_{1/2}$ mean values (\pm S.E.) are shown.



anti-MUC5AC antiserum⁴ (41). As shown in Fig. 5A (*top gel*), reduction of control extracts with DTT resulted in the detection of two major high molecular weight bands (lane 1), which likely corresponded to O-glycosylated and non-O-glycosylated reduced MUC5AC monomers, respectively (46). MUC5AC-62 antiserum did not recognize any protein band from unreduced control extracts (lane 2). In contrast, in protein extracts from cells previously incubated with 1 mM (lane 3) or 5 mM THP (lane 4), MUC5AC-062 antiserum recognized the two MUC5AC species detected in protein extracts reduced with DTT (lane 1). In addition, a smear, which might correspond to partially reduced forms of MUC5AC oligomers/multimers, appeared when cells were incubated with 5 mM THP (lane 4) but not with 1 mM THP (lane 3) or when control proteins were reduced with DTT (lane 1). These results showed that THP reduced intra- and interchain disulfide bonds in MUC5AC and likely other mucins and cystine-containing proteins.

Reblotting of the same nitrocellulose membranes with the monoclonal antibody MUC5AC 2Q445, which only recognizes non-O-glycosylated MUC5AC species irrespective of its oxidation state, clearly increased the signal of the faster migrating MUC5AC forms in DTT- (lane 1, *bottom gel*) and THP-reduced samples (lanes 3 and 4, *bottom gel*). These results confirmed that the faster migrating MUC5AC species were non-O-glycosylated monomers. In addition, this antibody also recognized two protein bands in the unreduced control sample (lane 2, *bottom gel*), which likely corresponded to non-O-glycosylated dimeric and monomeric forms with intact intradisulfide bonds that prevented their recognition by MUC5AC 062 antiserum. These results were not surprising because disulfide-linked dimerization of gel-forming mucin occurs in the endoplasmic reticulum prior to O-glycosylation in the Golgi complex (6). It can be concluded, therefore, that intra- and inter-

chain disulfide bonds in intragranular mucins were reduced during the incubation of the cells with THP.

When observed with the confocal microscope, THP-incubated living mucous cells were similar to those in control cells with numerous, highly fluorescent granules (Fig. 5B). FRAP analysis showed that the intragranular SHGFP-MUC5AC/CK was fractionated between the immobile matrix and the fluid phase, but the concentration in the mobile fraction was significantly reduced (Fig. 5, C and D). Indeed, SHGFP-MUC5AC/CK had an intragranular M_f average value of 12.23 \pm 2.38% compared with 44 \pm 1.98% in mucin granules of control cells analyzed in parallel. These data showed that intraluminal inter- and intrachain disulfide bonds were not required to maintain the intragranular organization. Hence, these results support the notion that electrostatic bonds between sulfated/sialylated mucins and multivalent cations, rather than interchain disulfide links and/or noncovalent protein-protein interactions among mucins, are largely responsible for holding the intragranular mucin matrix together (16, 17).

Nevertheless, the results did not disprove that specific protein-protein interactions could be important in mucin matrix condensation, during the early stages of biogenesis of the granule, when the pH is less acidic. To test this possibility, we carried out FRAP studies in mucous cells incubated with DTT, a well established, membrane-permeable disulfide reductant effective near neutral pH (37), in the presence of bafilomycin A₁. Bafilomycin A₁ is a specific inhibitor of the vacuolar H⁺-ATPase that maintains the acidic pH in secretory granules (36), and likely the mucin granules, as judged by immunofluorescence studies in fixed cells (see supplemental Fig. S3). It is important to notice that incubation of mucous cells with bafilomycin A₁ alone resulted in a \sim 20% increase in the mean value of SHGFP-MUC5AC/CK M_f and, often, granules with irregular intraluminal fluorescence distribution (26).

⁴ J. Perez-Vilar and R. Mabolro, unpublished observations.

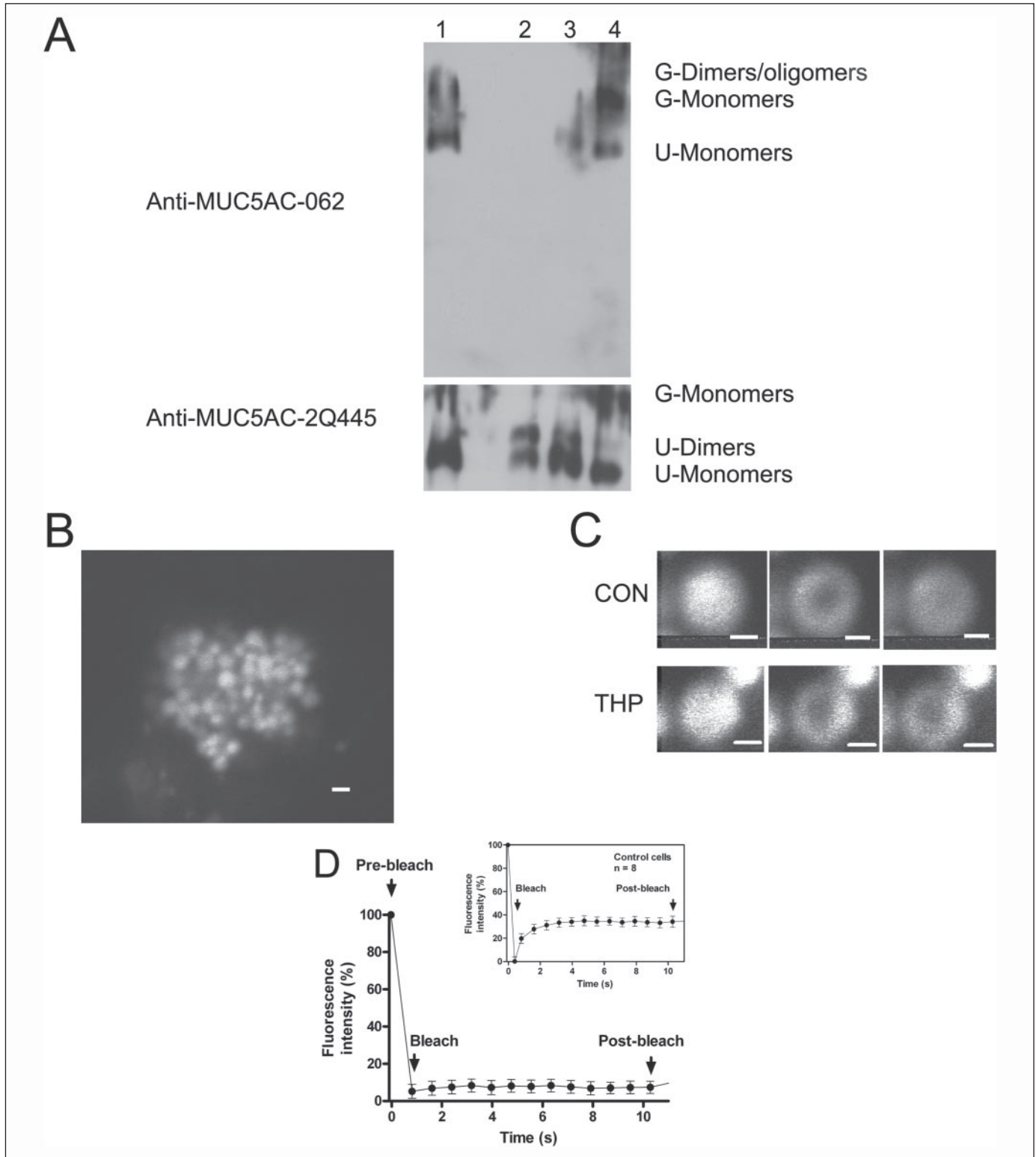
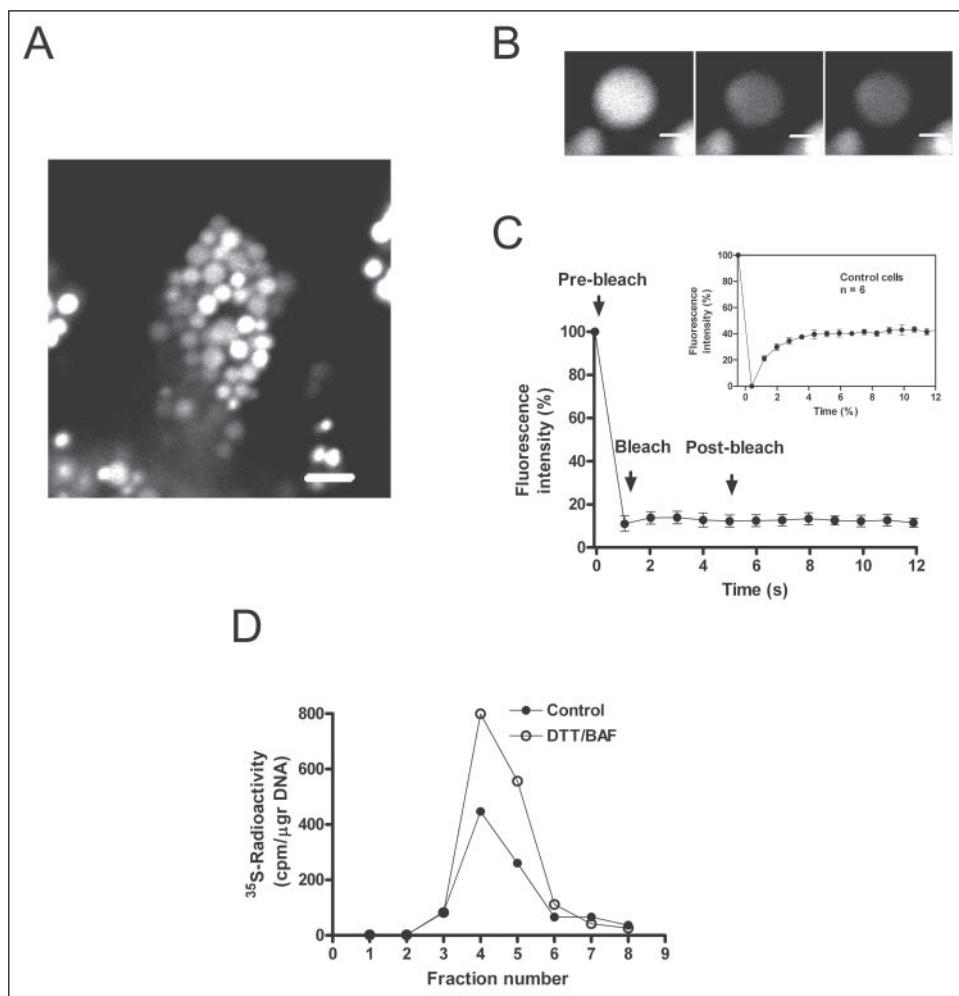


FIGURE 5. Mobile fraction and mobility of intragranular SHGFP-MUC5AC/CK in live mucous cells incubated with THP. *A*, cellular proteins of mucous cells previously incubated with vehicle (*lanes 1 and 2*), 1 mM THP (*lane 3*), or 5 mM THP (*lane 4*) were separated in agarose gels with (*lane 1*) or without (*lanes 2–4*) prior reduction of disulfide bonds with DTT. The proteins were transferred to nitrocellulose membranes and detected with anti-MUC5AC 062 rabbit antiserum (*top blot*) and then reblotted with anti-MUC5AC 2Q445 mouse monoclonal (*bottom blot*). Positive bands were detected by chemiluminescence. *G-Dimers/Oligomers*, O-glycosylated disulfide-linked MUC5AC dimers/oligomers; *G-Monomers*, O-glycosylated MUC5AC monomers; *U-Monomers*, MUC5AC monomers without O-linked oligosaccharides; *U-Dimers*, MUC5AC dimers without O-linked oligosaccharides. *B*, *xy* confocal image of a representative living mucous cell incubated for 4 h in the presence of THP. Scale bar = 2 μ m. *C*, a mucin granule in a representative control (CON) or THP-treated live goblet cell, showing pre- (*left*), immediately post- (*center*), and 10 s postbleaching (*right*) confocal images. Scale bar = 0.5 μ m. *D*, averaged (mean \pm S.E.) normalized FRAP bleaching/recovery curves for eight granules in different control (*top right inset*) or THP-incubated goblet/mucous cells. Error bars indicate S.E.

Mucin Granule Intraluminal Organization

FIGURE 6. Mobile fraction and mobility of intragranular SHGFP-MUC5AC/CK in live mucous cells incubated with bafilomycin A₁/DTT. *A*, *xy* confocal image of a representative bafilomycin A₁/DTT-treated live mucous/goblet cell. Scale bar = 2 μm. *B*, a representative mucin granule in a DTT/bafilomycin-incubated mucous cell, showing pre- (left), immediately post- (center), and 5 s post-bleaching (right) confocal images. Scale bar = 0.5 μm. *C*, averaged (mean ± S.E.) normalized FRAP bleaching/recovery curves for six granules in different control (top right inset) and bafilomycin A₁/DTT-treated goblet/mucous cells. Error bars indicate S.E. *D*, representative result of studies assessing the incorporation of [³H]GlcNAc into secreted proteins of control (CON) or bafilomycin/DTT-incubated (DTT/BAF) HT29-SHGFP-MUC5AC/CK cells. After the metabolic labeling with [³H]GlcNAc, proteins in the culture medium were fractionated in a Sephadex G-50 column, the radioactivity (cpm) in each fraction was determined, and the results were divided by the total DNA in the respective cell extracts.



Cultures incubated with both DTT and bafilomycin presented mucous/goblet cells with abundant granules and intense intragranular fluorescence (Fig. 6A), which appeared homogeneously distributed. Granules with heterogeneous distribution of luminal fluorescence, like those observed in bafilomycin-treated cells (26), were infrequent. Contrary to granules in control, bafilomycin- (26) or THP-treated cells, photobleaching of bafilomycin/DTT-exposed granules resulted in an almost immediate redistribution and sudden decrease of SHGFP-MUC5AC/CK intragranular fluorescence (Fig. 6B) and, accordingly, bleaching curves with virtually no recovery of fluorescence (Fig. 6C). The absence of a bleach spot suggested that intragranular SHGFP-MUC5AC/CK diffused very rapidly (38). In addition, the sudden reduction in the whole granule fluorescence intensity is consistent with diminished intragranular concentration of the GFP fusion protein compared with control, DTT- (not shown), bafilomycin- (26), or THP-exposed granules (Fig. 5B) (38). Partial secretion of the granules, therefore, would explain these observations.

This possibility of partial secretion of granule contents was investigated by determining the secretion of [³H]GlcNAc-labeled proteins from control or bafilomycin/DTT-treated cells. In these studies, mucous cells were radiolabeled with [³H]GlcNAc for 24 h, washed with PBS, and incubated for 4 h in unlabeled culture medium containing or not bafilomycin/DTT. ³H-Labeled glycoproteins in the culture medium were collected by gel filtration and the radioactivity measured in the exclusion volume fractions. As shown Fig. 6D, secretion of ³H-labeled glycoproteins increased ~1.7-fold in bafilomycin/DTT-treated cells

over control cells. These results suggest that reduction of intragranular disulfide bonds at neutral pH resulted in secretion of intracellular glycoproteins, consistent with the FRAP studies described above.

ATP Alters Mucin Granule Intraluminal Organization—Two potentially important concepts can be derived from the studies with bafilomycin/DTT described above. First, an alteration of the intraluminal organization (*i.e.* the immobile mucin matrix) could lead to accelerated mucin granule discharge. Second, an intact immobile matrix was not an absolute requisite to have morphologically normal granules. In view of these two possibilities, we decided to assess by FRAP analysis the intraluminal environment in granules of cells exposed to ATP, an established mucin secretagogue. We have shown before that in HT29-SHGFP-MUC5AC/CK cells, SHGFP-MUC5AC/CK is discharged from mucin granules within minutes of adding ATP (26). However, in these studies, it was also apparent that in many of these mucous cells not all of the SHGFP-MUC5AC/CK-containing granules disappeared after the addition of secretagogue. Moreover, a significant fraction of the goblet cells apparently was unresponsive to ATP. The reason for this heterogeneous response to ATP has not been yet investigated, but it may be related to the presence of goblet cells at different stages of their maturation process, secretagogue degradation, and/or perhaps an inherent genetic limitation (*i.e.* low P2Y₂ receptor expression) of the carcinoma cell line used. It must be noticed, however, that incomplete discharge of mucous cells upon the addition of secretagogue has been reported in the past in more physiological relevant model systems (*e.g.* 47).

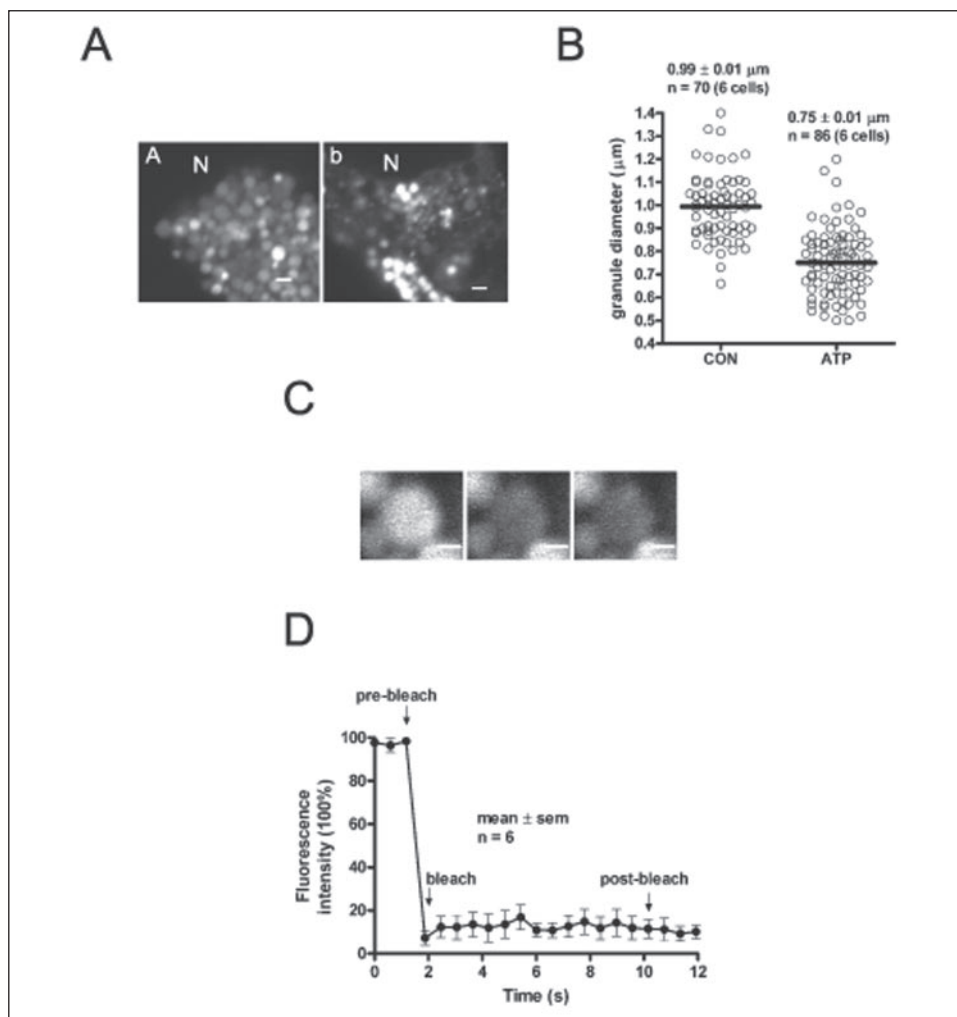


FIGURE 7. Mobile fraction and mobility of intragranular SHGFP-MUC5AC/CK in live mucous cells incubated with ATP. *A*, xy confocal images of a representative goblet/mucous cell before (*a*) or 30 min after the addition of ATP (*b*). *N*, nucleus. Scale bar = 1 μm . *B*, scatter plot of mucin granule diameters in control (CON) and ATP-treated live mucous/goblet cells. The respective mean values (\pm S.E.) are shown. *C*, a representative mucin granule in an ATP-treated live goblet cell, showing pre- (left), immediately post- (center), and 14 s post-bleaching (right) confocal images, is shown at the top. Scale bar = 0.5 μm . *D*, averaged (mean \pm S.E.) normalized FRAP bleaching/recovery curve for six granules in different ATP-treated goblet/mucous cells. Error bars indicate S.E.

For these studies, live mucous cells were incubated in the presence of ATP and observed 30 min later via confocal microscopy. Mucous/goblet cells with granules larger than 1.1 μm in diameter were identified and analyzed by FRAP. Fig. 7A shows the granular mass of one of these cells just before (*a*) and after the addition of ATP (*b*). The number of fluorescent granules diminished after the addition of ATP, consistent with total lumen discharge of a fraction of them (26). Nevertheless, many of the granules still had intraluminal fluorescence, which indicated incomplete or no SHGFP-MUC5AC/CK secretion. In addition, the differences in the sizes of control and ATP-incubated granules were statistically significant ($p < 0.001$; Fig. 7B), consistent with partial granule discharge. FRAP studies corroborated this initial assessment. First, the whole granule intraluminal fluorescence diminished rapidly and virtually did not recover afterward (Fig. 7C). Second, a bleach spot was not observed, and, accordingly, the FRAP curves showed the absence of a recovery phase (Fig. 7D). These results suggest the existence of highly mobile, but quantitatively limited, SHGFP-MUC5AC/CK in postexocytosis mucin granules.

DISCUSSION

The intragranular SHGFP-MUC5AC/CK FRAP parameters M_f and $t_{1/2}$ give a direct assessment in living mucous cells of the relationship between the fusion protein and the granule (mucin) matrix and, indirectly, of its organization (26, 38). Reduction of mucin-type *O*-glycans increased both SHGFP-MUC5AC/CK intragranular mobility and its

binding to the mucin matrix (Fig. 2). Three major albeit tentative conclusions can be drawn from these results. First, SHGFP-MUC5AC/CK binds to protein, rather than to *O*-glycan-rich, regions of the granule matrix. For instance, the MUC5AC/CK domain in the fusion protein could be interacting noncovalently with its native counterpart or other protein domain in intragranular mucins. Second, steric hindrance by mucin-type *O*-glycans likely prevents binding of the fusion protein/secretory proteins to the mucin matrix, *i.e.* to the unglycosylated matrix proteins. This conclusion is also supported by the observation that inhibition of sialylation, one of the most important modifications in mucin-type *O*-glycans, also decreased SHGFP-MUC5AC/CK mobile fraction (Fig. 4). Third, mucin-type *O*-glycans limit the diffusion of secretory proteins through the granule fluid compartment. Mucin intragranular matrix is likely forming a meshwork in which proteins move very slowly ($\leq 0.01 \mu\text{m}^2 \text{s}^{-1}$) through its pores (26). Collisions with mobile and immobile proteins and with mucin *O*-glycans in the matrix meshwork pores are expected to influence protein intragranular diffusion, as suggested by studies addressing protein diffusion inside cell compartments (48). Moreover, on the basis of their dipolar nature, water molecules could form organized layers around acidic groups of *O*-glycans, increasing the intragranular viscosity (49). Indeed, SHGFP-MUC5AC/CK intragranular mobility increased from inhibition of protein sulfation (Fig. 3). Because mucin-type *O*-glycans appear to be undersulfated in HT29-SHGFP-MUC5AC/CK cells (Fig. 3F), sulfate groups in high molecular weight, xylose-containing proteoglycans (Fig. 3, E and F)

Mucin Granule Intraluminal Organization

might contribute to limit protein intragranular diffusion. Nevertheless, although heparan sulfate is known to be expressed in HT29 cells (50), the existence of intragranular proteoglycans in mucous/goblet cells remains unproven.

Contrary to inhibition of sulfation, reduced sialylation diminished SHGFP-MUC5AC/CK intragranular mobility. These apparently conflicting results can be explained by considering the regulation of mucin-type *O*-glycosylation biosynthesis. Thus the control of the elongation and termination of mucin-type *O*-glycans largely involves competition among different families of enzymes, especially sialyl-, fucosyl-, and sulfotransferases (44, 51, 52). The specific combination of these enzymes and the relative levels of expression of each one of their members dictate the types and abundance of mucin type *O*-glycans. In the case of mucous HT29 cell strains, short sialylated *O*-glycan chains, among them the trisaccharide T/S-GalNAc-Gal-SiaNAc, are predominant (53). Hence, inhibition of mucin sialylation would likely produce an excess of mucin precursors with type 1 core structures, *i.e.* T/S-GalNAc-Gal. This disaccharide could be further elongated or, alternatively, modified into the type 2 core T/S-GalNAc-(GlcNAc)-Gal, another of the core structures detected in HT29 cells (53), which would be also available for further elongation. Ultimately, larger *O*-glycan chains will increase the hydrodynamic hindrance on and impose a physical obstruction to the intragranular secretory proteins, explaining the reduction in SHGFP-MUC5AC/CK GFP M_j and its mobility.

Besides the high degree of *O*-glycosylation, gel-forming mucins are characterized by the formation of disulfide-linked oligomers/multimers (6). The protein domains involved in mucin multimerization are rich in cysteine residues and lack *O*-glycans (6). Disruption of disulfide bonds at the acidic pH of the mucin granule lumen did not alter mucous cell/mucin granule morphology except that the SHGFP-MUC5AC/CK mobile fraction virtually disappeared (Fig. 5). Novel interactions between the reduced, likely unfolded, fusion protein and unglycosylated cysteine-rich domains of the endogenous mucins could explain these observations. In any case, it can be concluded that mucin covalent oligomerization/multimerization is not required to maintain the condensed intragranular mucin matrix, at least, once the granules are assembled as suggested earlier (16, 17). Physical interactions in the context of the intragranular environment, *i.e.* acidic pH and high concentrations of multivalent cations, seem to be sufficient to hold the matrix meshwork.

Yet, reduction of intragranular disulfide bonds at neutral pH profoundly disorganized the granule lumen and, eventually, resulted in granule discharge (partial) and also in the disappearance of the immobile fraction (Fig. 6). In line with previous studies (16, 17, 26, 54), these results give further support to the notion that intragranular acidic pH is crucial for mucin matrix intragranular condensation. Most important, these results also suggest that interactions involving folded proteins (*i.e.* with native disulfide bonds) are relevant for the matrix condensation mechanism albeit at an early stage, when the pH is less acidic, and prior to completion of mucin granule maturation. In this respect, *trans*-Golgi compartments and immature granules, the two organelles where granule matrix condensation might commence, have less acidic intraluminal pH than the mature granule (2, 3, 55).

Mucins are secreted by a poorly characterized Ca^{2+} -dependent mechanism, which recent studies suggest is modulated by the myristoylated, alanine-rich protein kinase C substrate (MARCKS) (56, 57). By interacting with the actin cytoskeleton and the mucin granule membrane, MARCKS might direct the granules to docking sites on the cell membrane. We have shown that mucin granule exocytosis can be triggered by altering the intragranular matrix organization, in our case

increased intraluminal pH and chemical reduction of intragranular cysteine residues (Fig. 6). These results suggest that one of the early steps during mucin-regulated secretion, prior to mucin granule trafficking and docking, is a change in the granule intraluminal organization. This concept is not novel. For instance, it has been proposed that a Ca^{2+} -dependent intragranular alkalinization of secretory granules of PC12 cells precedes exocytosis (58). Moreover, secretory granule swelling has been reported prior to exocytosis in pancreatic acinar cells (59). Although increased intraluminal pH might be a functional alteration during the perfusion phase of mucin granule exocytosis, reduction of disulfide bonds is less likely to be present. In fact, proof of disulfide reduction prior to or during secretory granule exocytosis in any cell type is lacking.

Although simple exocytosis can result in total fusion of the granule with the cell membrane, it is increasingly clear that in many cell types, secretory granules can be retrieved in one piece after exocytosis (4, 60). Thus, the secretory granules/vesicles transiently dock and fuse with the cell membrane, discharging none, part, or all of their cargo and, hence, form in the process intact, partially, or totally empty secretory granules/vesicles, respectively (*e.g.* 60–62). Our results with bafilomycin/DTT (Fig. 6) and the mucin secretagogue ATP (Fig. 7) clearly suggested the presence of partially discharged granules with limited SHGFP-MUC5AC/CK and likely no intragranular matrix. Hence, these results support the notion that transient simple exocytosis, rather than massive compound exocytosis (63) or apocrine secretion (64), is prevalent in HT29-SGFP-MUC5AC/CK cells under the conditions assayed. Such a mechanism would suggest that the decondensation and expansion of the mucin matrix take place extracellularly, either as the matrix traverses the fusion pore or shortly thereafter.

In summary, the mucin granule lumen is organized into a pH-dependent immobile, condensed (mucin) meshwork embedded in a mobile or fluid phase where proteins very slowly diffuse (26). Charge density (*i.e.* the degree of mucin sialylation and sulfation) of the mucin matrix and other intragranular glycoproteins, and also the length of their *O*-glycans, determine the mobility of secretory proteins through the matrix pores. Mucin *O*-glycans also affected the accessibility of secretory products to protein binding regions. Intraluminal acidic pH, together with the high concentration of multivalent cations, maintains the condensed meshwork via noncovalent interactions. This is irrespective of the degree of mucin matrix covalent multimerization and likely folding state. However, interactions among cysteine-rich domains in mucins are required during the early stages of mucin matrix condensation.

Acknowledgments—We thank Prof. C. Thorpe (Dept. of Chemistry and Biochemistry, University of Delaware) for suggesting to us the use of THP and Drs. M. Chua and W. Salmon (Michael Hooker Microscopy facility, University of North Carolina at Chapel Hill) for assistance with confocal microscopy procedures.

REFERENCES

1. Kepes, F., Rambourg, A., and Satiat-Jeunemaitre, B. (2005) *Int. Rev. Cytol.* **242**, 55–120
2. Burgoyne, R. D., and Morgan, A. (2003) *Physiol. Rev.* **83**, 581–632
3. Thiele, C., and Huttner, W. B. (1998) *Cell Dev. Biol.* **9**, 511–516
4. Strous, G. J., and Dekker, J. (1992) *Crit. Rev. Biochem.* **27**, 57–92
5. Gendler, D. J., and Spicer, A. P. (1995) *Annu. Rev. Physiol.* **57**, 607–634
6. Perez-Vilar, J., and Hill, R. L. (1999) *J. Biol. Chem.* **274**, 31751–31754
7. Dekker, J., Rossen, J. W., Buller, H. A., and Einerhand, A. W. (2002) *Trends Biochem. Sci.* **27**, 126–131
8. Basbaum, C., Lemjabbar, H., Longphre, M., Li, D., Gensch, E., and McNamara, N. (1999) *Am. J. Respir. Crit. Care Med.* **160**, S44–S48
9. Knowles, M. R., and Boucher, R. C. (2002) *J. Clin. Invest.* **109**, 571–577
10. Perez-Vilar, J., and Boucher, R. C. (2004) *Free Rad. Biol. Med.* **37**, 1564–1577

11. Wickstrom, C., and Carlstedt, I. (2001) *J. Biol. Chem.* **276**, 47116–47121
12. Lidell, M. E., Johansson, M. E., and Hansson, G. C. (2003) *J. Biol. Chem.* **278**, 13944–13951
13. Perez-Vilar, J., Randell, S. H., and Boucher, R. C. (2004) *Glycobiology* **14**, 325–337
14. Neutra, M. R., Phillips, T. L., and Phillips, T. E. (1984) *CIBA Found. Symp.* **109**, 20–39
15. Rogers, D. F. (2003) *Int. J. Biochem. Cell Biol.* **35**, 1–6
16. Verdugo, P. (1990) *Annu. Rev. Physiol.* **52**, 157–176
17. Verdugo, P. (1991) *Am. Rev. Respir. Dis.* **144**, S33–S37
18. Velcich, A., Yang, W., Heyer, J., Fragale, A., Nicholas, C., Viani, S., Kucherlapati, R., Lipkin, M., Yang, K., and Augenlicht, L. (2002) *Science* **295**, 1726–1729
19. Serafin, W. E., Katz, H. R., Austen, K. F., and Stevens, R. L. (1986) *J. Biol. Chem.* **261**, 15017–15021
20. Day, R., and Gorr, S. U. (2003) *Trends Endocrinol. Metab.* **14**, 10–13
21. Chin, W. C., Orellana, M. V., Quesada, I., and Verdugo, P. (2004) *Plant Cell Physiol.* **45**, 535–542
22. Tanaka, T., and Filmore, D. J. (1979) *J. Chem. Phys.* **70**, 1214–1220
23. Verdugo, P. (1984) *CIBA Found. Symp.* **109**, 212–225
24. Marszalek, P. E., Farrell, B., Verdugo, P., and Fernandez, J. M. (1997) *Biophys. J.* **73**, 1160–1168
25. Marszalek, P. E., Farrell, B., Verdugo, P., and Fernandez, J. M. (1997) *Biophys. J.* **73**, 1169–1183
26. Perez-Vilar, J., Olsen, J. C., Chua, M., and Boucher, R. C. (2005) *J. Biol. Chem.* **280**, 16868–16881
27. Perez-Vilar, J., Ribeiro, C. M., Salmon, W. C., Mabolro, R., and Boucher, R. C. (2005) *J. Histochem. Cytochem.* **53**, 1305–1308
28. Nguyen, T., Chin, W. C., and Verdugo, P. (1998) *Nature* **395**, 908–912
29. Quesada, I., Chin, W. C., and Verdugo, P. (2003) *Biophys. J.* **85**, 963–970
30. Deleted in proof
31. Hang, H. C., Yu, C., Ten Hagen, K. G., Tian, E., Winans, K. A., Tabak, L. A., and Bertozzi, C. R. (2004) *Chem. Biol.* **11**, 337–345
32. Dekker, J., Van Beurden-Lamers, W. M., and Strous, G. J. (1989) *J. Biol. Chem.* **264**, 10431–10437
33. Lohmander, L. S., Hascall, V. C., and Caplan, A. I. (1979) *J. Biol. Chem.* **254**, 10551–10561
34. Lee, K. Y., Kim, H. G., Hwang, M. R., Chae, J. L., Yang, J. M., Lee, Y. C., Choo, Y. K., Lee, Y. I., Lee, S. S., and Do, S. I. (2002) *J. Biol. Chem.* **277**, 49341–49351
35. Cline, D. J., Redding, S. E., Brohawn, S. G., Psathas, J. N., Schneider, J. P., and Thorpe, C. (2004) *Biochemistry* **43**, 15195–15203
36. Drose, S., and Altendorf, K. (1997) *J. Exp. Biol.* **200**, 1–8
37. Braakman, I., Helenius, J., and Helenius, A. (1992) *EMBO J.* **11**, 1717–1722
38. Snapp, E., Altan, N., and Lippincott-Schwartz, J. (2003) in *Current Protocols in Cell Biol.* (Bonifacino, J., Dasso, M., Harford, J., Lippincott-Schwartz, J., Yamada, K., and Morgan, K. S., eds) John Wiley & Sons, Inc., New York
39. Philips, T. E., Ramos, R., and Duncan, S. L. (1995) *In Vitro Cell Dev. Biol. Anim.* **31**, 421–423
40. Thornton, D. J., Howard, M., Devine, P. L., and Sheehan, J. K. (1995) *Anal. Biochem.* **227**, 162–167
41. Sheehan, J. K., Brazeau, C., Kutay, S., Pigeon, H., Kirkham, S., Howard, M., and Thornton, D. J. (2000) *Biochemistry* **347**, 37–44
42. Tian, E., Hagen, K. G., Shum, L., Hang, H. C., Imbert, Y., Young, W. W., Jr., Bertozzi, C. R., and Tabak, L. A. (2004) *J. Biol. Chem.* **279**, 50382–50390
43. Wang, Z. B., Liu, Y. Q., and Cui, Y. F. (2005) *Cell Biol. Int.* **29**, 489–496
44. Brockhausen, I. (2003) *Biochem. Soc. Trans.* **31**, 318–325
45. Kitamura, H., Cho, M., Lee, B. H., Gum, J. R., Siddiki, B. B., Ho, S. B., Toribara, N. W., Lesuffleur, T., Zweibaum, A., Kitamura, Y., Yonezawa, S., and Kim, Y. S. (1996) *Eur. J. Cancer* **32A**, 1788–1796
46. Sheehan, J. K., Kirkham, S., Howard, M., Woodman, P., Kutay, S., Brazeau, C., Buckley, J., and Thornton, D. J. (2004) *J. Biol. Chem.* **279**, 15698–15705
47. Halm, D. R., and Halm, S. T. (2000) *Am. J. Physiol.* **278**, C212–C233
48. Periasamy, N., and Verkman, A. S. (1998) *Biophys. J.* **75**, 557–567
49. Pollack, G. H. (2003) *Adv. Colloid. Interface Sci.* **103**, 173–196
50. Molist, A., Romaris, M., Lindahl, U., Villena, J., Touab, M., and Bassols, A. (1998) *Eur. J. Biochem.* **254**, 371–377
51. Hanisch, F. G. (2001) *Biol. Chem.* **382**, 143–149
52. Spiro, R. G. (2002) *Glycobiology* **12**, 43R–56R
53. Gouyer, V., Leteurtre, E., Zanetta, J. P., Lesuffleur, T., Delannoy, P., and Huet, G. (2001) *Front. Biosci.* **1**, D1235–D1244
54. Espinosa, M., Noe, G., Troncoso, C., Ho, S. B., and Villalon, M. (2002) *Hum. Reprod.* **17**, 1964–1972
55. Tooze, S. A., Martens, G. J., and Huttner, W. B. (2001) *Trends Cell Biol.* **11**, 116–122
56. Li, Y., Martin, L. D., Spizz, G., and Adler, K. B. (2001) *J. Biol. Chem.* **276**, 40982–40990
57. Singer, M., Martin, L. D., Vargaftig, B. B., Park, J., Gruber, A. D., Li, Y., and Adler, K. B. (2004) *Nat. Med.* **10**, 193–196
58. Han, W., Danqing, L., Stout, A. K., Takimoto, K., and Levitan, E. S. (1999) *J. Neurosci.* **19**, 900–905
59. Kelly, M. L., Cho, W. J., Jeremic, A., Abu-Hamdah, R., and Jena, B. P. (2004) *Cell Biol. Int.* **28**, 709–716
60. Palfrey, H. C., and Artalejo, C. R. (2003) *Curr. Biol.* **13**, R397–R399
61. Taraska, J. W., Perrais, D., Ohara-Imaizumi, M., Nagamatsu, S., and Almers, W. (2003) *Proc. Natl. Acad. Sci. U. S. A.* **100**, 2070–2075
62. Aravanis, A. M., Pyle, J. L., and Tsien, R. W. (2003) *Nature* **423**, 643–647
63. Specian, R. D., and Oliver, M. G. (1991) *Am. J. Physiol.* **260**, 183–193
64. Puchelle, E., Beorchia, A., Menager, M., Zahm, J. M., and Ploton, I. (1991) *Biol. Cell* **72**, 159–166